



25th International Meshing Roundtable (IMR25)

A 3D Constrained Optimization Smoother to post-process Quadrilateral Meshes for Body-In-White

Nilanjan Mukherjee^{a*}, Jonathan E. Makem^b, Harold J. Fogg^b

Meshing & Abstraction, Digital Factory, Simulation and Test Solutions Siemens PLM Software, SIEMENS.

^a2000 Eastman Dr., Milford, Ohio 45150 USA

^bFrancis House, 112 Hills Road, Cambridge, UK. CB2 1PH

Abstract

Finite element analyses of 3D quadrilateral meshes for automotive body-in-white panels have stringent mesh quality requirements. Several mesh quality metrics, namely element included angles, minimum Jacobian determinant, skew, taper, warp, aspect ratio, minimum element length etc. need to be within acceptable limits. No constitutive relations exist that can tie all these parameters to a single metric that mesh post-processing can target. In the paper presented, a 3D optimization smoothing algorithm is proposed based on element included angles with the constraints of a minimum edge length and geometry fidelity envelope. A complex cost-function is set up for each element based on included element angle at the element corners. Element angle perturbation methods are devised to exercise local control on included angles of quadrilateral and mixed meshes. A minimization principle is worked out to reduce the cost function to an acceptable limit. Goal proximity is defined by acceptable error norms and ranges. Mesh nodes are repositioned iteratively but bound by a geometry fidelity envelope apart from the minimum element edge length constraint. Striking improvement in mesh quality statistics is reported with reasonably monotonic solution convergence patterns.

© 2015 The Authors. Published by Elsevier Ltd.

Peer-review under responsibility of organizing committee of the 25th International Meshing Roundtable (IMR25).

Keywords: optimization; smoothing; quadrilateral mesh; perturbation; included angles, edge length, cost function; skew; warp, taper, Jacobian ;

1. Introduction

According to industrial practice, automotive body-in-white meshes are almost always quadrilateral or hybrid (quad-dominant) and are typically generated by creating first a 2D mesh on surface parametric space which is

* Corresponding author. Tel.: +1 513 576-7026; fax: +0-000-000-0000 .

E-mail address: mukherjee.nilanjan@siemens.com

subsequently transformed into 3D. It has become customary in the automotive industry to subject these quadrilateral meshes to a plethora of element quality checks, namely – minimum Jacobian determinant, warp, taper, skew, quadrilateral and triangular (for quad-dominant meshes) minimum/maximum angle limits, aspect ratio and minimum element-edge length or MEL. Most of these checks are performed irrespective of the chosen solver. Quadrilateral mesh generation algorithms cannot be conditioned by such a large gamut of pressing quality requirements. Furthermore, it is extremely inefficient and non-trivial to evaluate these quality metrics and correcting the mesh in 3D space while generating it. There is thus a need in the meshing process to incorporate a mesh post-processing step where a variety of tools are used to modify element shapes so that they conform to the required quality limits. Unfortunately, no well-defined constitutive relations exist that can relate each one of these metrics to a single quality measure. On the contrary, some of these metrics can conflict with others. For example, while trying to fix warp, a post-processing algorithm might worsen element skew, min/max angles or taper.

2. Optimization smoothing of Quadrilateral meshes

In any optimization smoothing algorithm, a cost function is set up to define the metric pursued [1]. A minimization principle is also worked out to reduce the cost function to an acceptable limit. Goal proximity is usually managed by defining error norms and their acceptable ranges [2]. Thus, in an effort to minimize the cost function, the nodes of the mesh are repositioned either iteratively [1,2,3,4] or via quasi-static simultaneous equation solve systems [5]. Some traditional mesh smoothing cost functions include quality metrics like (a) Element Included Angles (Minimum/Maximum defining acceptable range), (b) Element Distortion Metrics, (c) Aspect Ratio [1, 2] etc. Element included angles are either maximized or minimized in order to eliminate severely distorted elements. Popularly used distortion metrics are defined either in terms of area and the edge length of elements or its angles. The use of non-dimensional mesh quality metrics is popular as they offer a good shape quality measure of an element in a neutral scale. An equilateral triangle (for triangles) and a square/rectangle (for quadrilaterals) are shown to possess the ideal values in that scale. The further an element distortion metric is from these ideal values, the more severely distorted it is. Compared to non-optimization smoothing methods (like Laplacian smoothing and its variants) optimization-based smoothing methods can guarantee the improvement of mesh quality. Optimizing the quality metrics, severely distorted elements can be effectively corrected. The degree of collective improvement depends on the computational cost one is willing to incur. Zhou and Shimada [4] observed for a two-dimensional triangular mesh, for example, optimization-based smoothing method can be five times more computationally expensive than smart Laplacian smoothing, a variation of Laplacian smoothing [2], and 30 to 40 times more computationally expensive than Laplacian smoothing. Knupp [6] has done a significant volume of work in the field of smoothing. In a series of investigations [6,7] Knupp laid the foundation for nodally based 2D and 3D objective functions using matrices and matrix norms. He showed how some of these objective functions can relate to the Jacobian matrix and how the condition number of the metric tensor objective functions in 2D failed to naturally extend to 3D. The objective functions were grouped to form weighted combinations and the condition number based objective function showed particular promise. In a later work Rao, Shashkov and Knupp [8] used a condition number based optimization smoothing algorithm for 3D surface meshes maintaining geometry fidelity by constructing element-based local parametric spaces.

Most of the optimization smoothing algorithms available in open literature, however, are performed in 2D and tend to focus more on triangular meshes than quadrilateral. No investigations were found on optimization smoothing on body-in-white quadrilateral and quad-dominant meshes in 3D. Need remains for an objective function that specifically targets automotive body panel meshes as the mesh quality goals are stringent.

3. Mesh quality challenges in Body-in-White

In the automotive industry, body-in-white (BIW) refers to the fabricated (usually seam and/or tack welded) sheet-metal components that form the car's body (shown in Figure 1). Body-in-white is a stage of the carbody prior to

painting and before the moving parts (doors, hoods, fenders etc.), the engine, chassis sub-assemblies, and trim (glass, seats, upholstery, electronics, etc.) have been mounted. Most of industrial body-in-white mesh generation is done using commercial software which either generate meshes in 2D parametric domains or in some rare cases directly on the 3D surface.

BIW meshes are typically bilinear quadrangular-dominant meshes as opposed to triangles. Linear triangles are constant-strain and tend to over-stiffen models which are subjected to a large number of structural analyses including transient dynamic and frequency response analysis. Consequently, mesh quality of quadrilateral and a small percentage of triangular elements used in these BIW models have stringent requirements and a single metric is usually not sufficient to measure it. There are additional constraints BIW meshes have to combat. The presence of loads and boundary conditions, pre-existing hard-points representing seam and tack welds are some of them. Crash analyses also limit the variation of element size in anisotropic meshes which is directly proportional to the time-step of quasi-static solutions. This makes the MEL perhaps the most important quality criterion for BIW meshes. Since most of the target element quality parameters are measured in 3D, a need arises for the mesh post-processor to address them in 3D. In the process mesh nodes are allowed to move off geometry in order to meet the stringent quality goals. Movement away from geometry must be limited though, which introduces another positional constraint – a geometric fidelity envelope (GFE) or tolerance. No node is allowed to move off geometry by an amount more than the GFE.

Several mesh quality parameters like skew, taper, warp, Jacobian determinant, element included angles, edge lengths and aspect ratio are used to measure distortion. Of these, with the exception of aspect ratio and warp, most other parameters are related to element angles in one way or another. Typically, for BIW quad-dominant meshes, the 3D angle limits for a quadrangular element are 50-150 deg., 40-140 deg. for triangles; minimum Jacobian ratio (min/max Jacobian determinant value) limit is 0.4, MEL is usually 0.4~0.6 times the global element size and the GFE is 0.2~0.4 times the global element size. Therefore, these meshes are usually generated either in 2D or 3D domains according to well-known meshing algorithms and sometimes smoothed and cleaned (typically in 2D parameter space) by elementary post-processing tools that are quick and do not target complex quality metrics. In our case, a variational smoother based on nodal valency [9] is used in 2D for each face to smooth the mesh. This improves the overall quality of the 2D mesh while maintaining perfect geometry fidelity, but it cannot target specific element quality. Thus, as a last step, a heavy-duty 3D post-processor becomes necessary to meet each and every single mesh quality metric.

In the present paper, an optimization based 3D quad-dominant mesh smoother is proposed for post-processing BIW meshes. The optimization smoother is angle-based. Its design variables are the positional coordinates of the nodes. The main objective is to minimize the collective distortion energy of the mesh resulting from element angular deviation with respect to an optimum shape. The objective or cost function is the deviation of element angle in 3D from an ideal target. This cost function is globally minimized. A non-dimensional element quality metric (EQM), defined in section 7, is used to control the smoother. The constraints for this optimization smoother are minimum element length or MEL as well as a geometry fidelity envelope or GFE.

The novel technique presented here demonstrates how the angle gradient may be used to improve element shape and minimize distortion in 3d surface meshes of industrial complexity. Unlike most authors who have reported on node-centered smoothing frameworks, this approach relies on a two-tiered element based configuration. A local solution is firstly achieved on an element-by-element basis and iteratively refined until a global solution is converged upon. By improving the included angles, other mesh metrics such as the Scaled Jacobian are enhanced and a mathematical relationship between the aforementioned quality measures is identified. Incorporating constraints such as MEL and GFE ensures the algorithm generates viable, functional meshes with enhanced quality characteristics.

4. 3D Element angle based optimization smoothing

If δ_i denotes the deviation of the nodes from an ideal configuration (in which all included angles of quadrilateral Q_i fall within desired limits) the distortion energy ε_i due to nodal deviation can be written as

$$\varepsilon_i = \frac{1}{2} \kappa_i \delta_i^2 \quad (1)$$

where κ_i is a stiffness constant and aggregate displacement δ_i can be expressed as

$$\delta_i = \sum_{j=1}^4 (\mathbf{X}_{optj} - \mathbf{X}_{0j}) \quad (1a)$$

for the i -th quadrilateral element and \mathbf{X}_{optj} represents the optimum location of element node j , while \mathbf{X}_{0j} is its initial position. The global distortion function Ψ for a mesh with N failing quad elements is given by

$$\Psi = \sum_{i=1}^N \frac{1}{2} \kappa_i \delta_i^2 \quad (2)$$

This global distortion function Ψ represents the objective or cost function for the problem posed. When Ψ is minimized, most or all elements in the mesh failing angle checks are reconfigured to passing angular limits. In order to minimize the global distortion energy with respect to the node coordinates \mathbf{X} (x, y, z) we arrive at

$$\frac{\partial \Psi}{\partial \mathbf{X}} = \sum_{i=1}^N \kappa_i \frac{\partial \delta_i}{\partial \mathbf{X}} = 0 \quad (3)$$

Equation (3) describes the global solution to the problem posed.

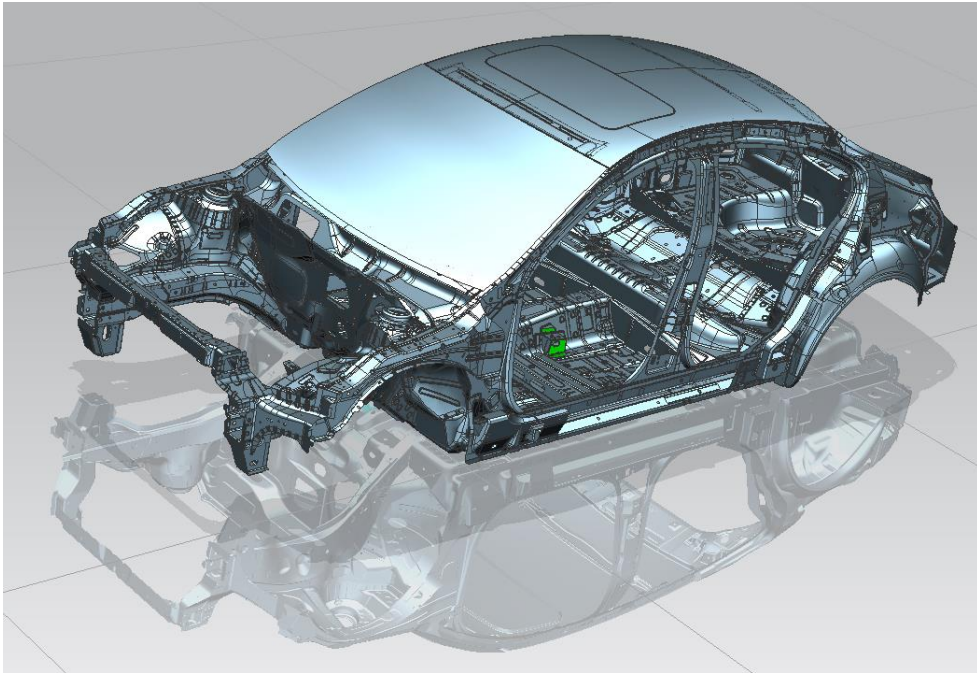
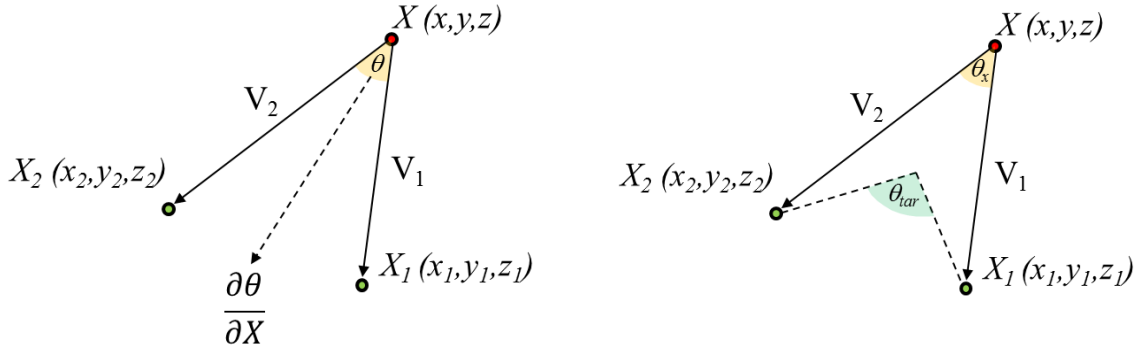


Fig. 1. A body-in-white representation of an Opel/Insignia model.

Large global problems are often ill-conditioned and likely to be awkward in terms of convexity. To get around this, we break down the global problem into a series of reduced problems that only involve the most dominant solution variables. These can be much more easily solved and convexity is easier to ensure. With each local solution at a node, which represents a discrete point in the field of the problem, we move incrementally towards the global solution. A local solution is required at the level of an element i to arrive at the optimum location for each one of its

j nodes. Figure 2(a) depicts one corner of a typical quadrilateral element. The angle θ is defined by the points X_1 , X and X_2 . Figure 3 shows how angle θ varies if the candidate node is moved holding its two connected nodes (X_1 and X_2) fixed at position $(0,0)$ and $(1,0)$. The closeness of the isolines imply the magnitude of the gradient. The magnitude of the gradient dramatically drops off at 180° . The direction of the gradient is always orthogonal to the isoline. Keeping X_1 and X_2 fixed, the gradient of this function w.r.t. X is a vector made up of partial derivatives. Its direction indicates the perturbation to X that will give the maximum change to the angle θ . Its magnitude indicates the rate of change of angle with respect to the perturbation length in said direction.



(a) angle gradient between 2 vectors in 3D space (b) nodal movement towards optimal configuration
 Fig. 2. Perturbation along the angle gradient.

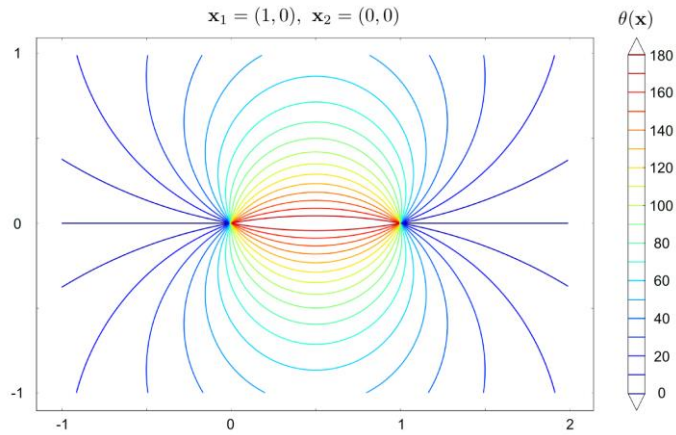


Fig. 3. Variation of angle θ with nodal position

$$V_1 = X_1 - X = ((x_1 - x), (y_1 - y), (z_1 - z)) \tag{4}$$

$$V_2 = X_2 - X = ((x_2 - x), (y_2 - y), (z_2 - z)) \tag{5}$$

$$\theta = \cos^{-1} \left(\frac{V_1 \cdot V_2}{|V_1| |V_2|} \right) \tag{6}$$

Substituting

$u = \frac{V_1 \cdot V_2}{|V_1| |V_2|} \dots 0 \leq u \leq 1$ in equation 6, one gets

$$\theta = \cos^{-1}(u) \tag{7}$$

Computing the partial derivatives of θ w.r.t. x

$$\frac{\partial \theta}{\partial x} = \frac{\partial}{\partial x} (\cos^{-1}(u)) = \frac{-1}{\sqrt{1-u^2}} \frac{\partial u}{\partial x} \quad (8)$$

leading further to

$$\begin{aligned} \frac{\partial u}{\partial x} &= \frac{\partial}{\partial x} \left(\frac{V_1 \cdot V_2}{|V_1| |V_2|} \right) \\ &= \frac{|V_1| |V_2| \frac{\partial}{\partial x} (V_1 \cdot V_2) - V_1 \cdot V_2 \frac{\partial}{\partial x} (|V_1| |V_2|)}{|V_1|^2 |V_2|^2} \end{aligned} \quad (9)$$

$$\frac{\partial}{\partial x} (V_1 \cdot V_2) = 2x - x_1 - x_2 \quad (10)$$

$$\frac{\partial}{\partial x} (|V_1| |V_2|) = \frac{(x-x_2) |V_1|^2 + (x-x_1) |V_2|^2}{|V_1| |V_2|} \quad (11)$$

Substituting equations 8 and 9 into equation 6 and adding the partial derivatives w.r.t. y and z yields

$$\begin{aligned} \nabla \theta(X) &= \frac{\partial \theta}{\partial X} = \left(\frac{\partial \theta}{\partial x}, \frac{\partial \theta}{\partial y}, \frac{\partial \theta}{\partial z} \right) \\ &= \frac{1}{\sqrt{1 - \left(\frac{V_1 \cdot V_2}{|V_1| |V_2|} \right)^2}} \left(|V_1|^2 |V_2|^2 (V_1 + V_2) - V_1 \cdot V_2 (|V_1|^2 V_2 + |V_2|^2 V_1) \right) \end{aligned} \quad (12)$$

Given the initial position of X is X_0 , the objective is to find the position X_{opt} . The cost function of the optimization problem thus reduces to the absolute difference between $\theta_{(X)}$, as shown in Figure 2(b) and target angle θ_{tar} , according to equation 14, where n is the number of element nodes..

$$f_{(X)} = |\theta_{(X)} - \theta_{tar}| \quad (13)$$

$$\text{where } \theta_{tar} = \pi - \frac{2\pi}{n} \quad (14)$$

In the problem thus posed, $X(x,y,z)$, the node coordinates define the design variables. The cost function defined by equation 13 is evaluated at each node of elements failing a target element quality metric. The constraints of this optimization problem are MEL and GFE. The element nodes are perturbed so as to minimize the cost function not only at each node, but more importantly idealize the quality metric for each element. As a given node is perturbed so as to improve a given angle of a defaulter element, it could, in the process, affect the included angles of all neighbor or connected elements. A global measure of errors thus becomes necessary. This global error norm is a measure of the change in cumulative distortion energy of the entire mesh. A steady and monotonic decay of the error norm is indicative of the rate at which the system reaches equilibrium.

5. Node perturbation method

After computing the angle gradient, it is necessary to determine the size of the perturbation along this vector to optimize the element quality metric or EQM. The premise of this approach is that the more orthogonal we make the angle, the smaller the deviation of the element quality metric from its ideal value. For very acute or obtuse angles which deviate greatly from 90°, the nodal perturbation will be more dramatic than nodes with included angles which are close to 90°. However, the objective is not to make every element a perfect rectangle as this is not viable in a global mesh, rather to strive towards an optimal configuration with improved orthogonality via incremental perturbation. Section 8 describes an approach which employs the magnitude of the angle gradient to intelligently predict the best perturbation per increment.

6. Optimization constraints

Certain BIW transient analyses (particularly crash) are performed as a set of quasi-static analysis as an approximation of a time-varying problem. The time step of these analyses of very large systems is extremely critical for the efficiency of vehicle design life cycle. The time step is a function of the smallest element edge length in the mesh and shrinks as the latter reduces, thus vastly increasing the number of analysis iterations performed for the entire vehicle. To avoid this analysis bloat, a critical minimum element length (MEL) becomes a mandatory lower limit of element size in the mesh. The MEL is defined as a lower threshold and no quadrilateral or triangular elements are supposed to violate it. Typically, the MEL is 30-67% of the global element size. This threshold serves as a constraint on the angle optimization smoother. Before moving any node to its predicted location, its distances from the adjacent connected nodes are checked to ensure MEL limit is not violated. If violated, the node is moved such that MEL is not violated as shown in Fig. 4a. The initial orange mesh is smoothed to the green state. Node A displaces to position B as a result, but in the process $d_g > MEL$. Hence, the node at A is displaced along the desired displacement vector \overline{AB} up to point C such that the new element length $d_b \leq MEL$. The blue elements show the final configuration.

In BIW analyses high fidelity geometry proximity for the mesh is unimportant. Nodes are allowed to move off geometry if required to satisfy the stringent quality criteria. However, there is a limit to this movement. This limit serves as the second constraint for angle optimization smoothing. The entire mesh can be allowed to move within a geometry fidelity envelope or tolerance (GFE) d_{mt} . This is achieved by allowing each node to move within a bound sphere of radius d_{mt} as shown in Fig. 4b. The node at position A would have been moved to location B by the smoother without this constraint. Instead, it is moved to location C traveling along vector \overline{AB} such that it is not out of bounds.

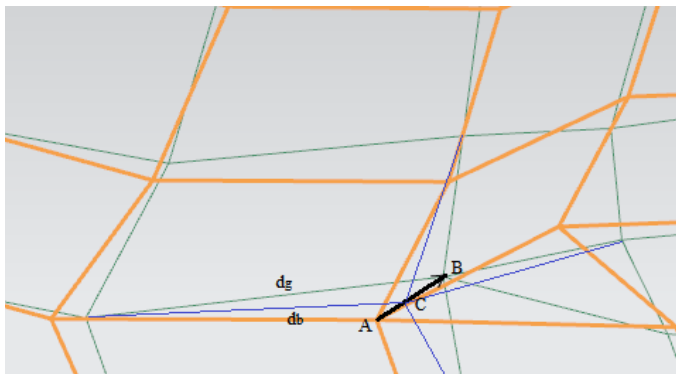


Fig. 4a. Displacement constraint due to MEL.

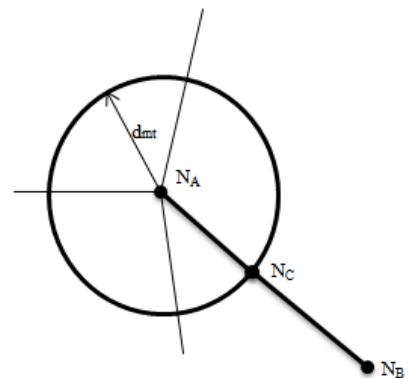


Fig. 4b. Displacement constraint due to GFE.

7. Element quality metric (EQM)

The non-dimensional metric, ε_θ used to evaluate the quality of each element is based on the root mean square (rms) of the deviation of the element included angles, $\theta_{i..n}$ from the optimum, θ_{tar} where n is the number of element nodes and δ_{rms} is the root mean square angular deviation.

$$\delta_{rms} = \sqrt{\frac{\sum_{i=0}^n (\theta_i - \theta_{tar})^2}{n}} \quad (15)$$

$$\varepsilon_\theta = \frac{1}{1 + \delta_{rms}} \quad (16)$$

The element quality metric defined in equation 16 is used as a limit which governs the convergence of the local solution, described in section 9.

The Scaled Jacobian [7, 10] $\det \bar{J}_i$ at the corner of an element is defined as the (signed) area of the parallelogram formed by the unitized edge vectors, \bar{V}_1 and \bar{V}_2 emanating from the corner, as shown in figure 2. Consequently, the Scaled Jacobian at a given node may be related to the included angle, θ_i according to equation 17.

$$\det \bar{J}_i = \|\bar{V}_1 \times \bar{V}_2\| = \|\bar{V}_1\| \|\bar{V}_2\| \sin \theta_i = \sin \theta_i \quad (17)$$

And therefore the included angle may be computed in terms of the Scaled Jacobian.

$$\theta_i = \sin^{-1}(\det \bar{J}_i) \quad (18)$$

So, for a given corner node of a quad element, as the included angle approaches 90° , the Scaled Jacobian approaches 1.0. Consequently, substituting equation 18 into 15 it is possible to redefine the element quality metric given in equation 16 in terms of the Scaled Jacobian as follows

$$\varepsilon_\theta = \frac{1}{1 + \sqrt{\frac{\sum_{i=0}^n (\sin^{-1}(\det \bar{J}_i) - \theta_{tar})^2}{n}}} \quad (19)$$

This proves that the element quality metric, ε_θ based on the angular deviation of the included angles from an optimum configuration is intrinsically linked to the Scaled Jacobian values at each corner node.

8. Solution Technique

The problem, as posed, calls for two solutions; the first one is local - at the level of each finite element failing the quality metric and finally a global solution for the entire mesh. In order to pursue an optimized solution at the local elemental level, we assume a local linear approximation to predict how $f(x)$ varies with the movement of X_0 as

$$f(x) \approx f(x_0) + f'(x_0) \tag{20}$$

$$\text{Where } f'(x_0) = \nabla f(x_0) = \left(\frac{\partial f(x_0)}{\partial x}, \frac{\partial f(x_0)}{\partial y}, \frac{\partial f(x_0)}{\partial z} \right) \tag{21}$$

Generally, the gradient of $f(x)$ is given by:

$$\nabla f(x) = \begin{cases} \nabla \theta(x), & \theta(x) > \theta_{tar} \\ -\nabla \theta(x), & \theta_{tar} > \theta(x) \end{cases} \tag{22}$$

The Newton-Raphson method can be employed to find the root of $f(x)$ and thus approximate the perturbation required to make $f(x) = 0$.

$$f(x_0) + f'(x_0)(X_1 - X_0) = 0 \tag{23}$$

$$\text{Let } \Delta X = (X_1 - X_0) \tag{24}$$

$$f'(x_0) \cdot \Delta X = -f(x_0) \tag{25}$$

As equation 22 describes an underdetermined linear system, we can solve for the least norm solution ΔX by taking the pseudo-inverse of $f'(x_0)$.

$$\Delta X = - \underbrace{f'(x_0)^T (f'(x_0) f'(x_0)^T)^{-1}}_{\text{pseudoinverse}} f(x_0) \tag{26}$$

Substituting equation 12 into 23 reduces to

$$\Delta X = - \frac{\nabla f(x_0)}{|\nabla f(x_0)|^2} f(x_0) \tag{27}$$

Substituting equation 10 and 13 into 24 further reduces to

$$\Delta X = - \frac{\nabla \theta(x_0)}{|\nabla \theta(x_0)|^2} (\theta(x_0) - \theta_{tar}) \tag{28}$$

As the objective is to move incrementally towards an orthogonal configuration, the perturbation will be a fraction S of ΔX according to equation 26.

$$X_{opt} = X_0 + S \Delta X \dots 0 < S < 1 \tag{29}$$

Equation (29) provides the local solution yielding a new, optimized location for each of the 4 nodes of the failing quadrilateral element.

9. Solution convergence

The problem posed calls for two levels of solutions – one at a local or elemental level described by equation (29) and another at a global or mesh level defined by equation (3). Equation (29) is solved for each element by nodal perturbation until the EQM $\epsilon_0 < \epsilon_{01}$ where ϵ_{01} is the cut-off limit. While nodes are perturbed for an element, typically that can affect neighboring elements, which in turn can begin to fail. This is covered by the global solution.

In a typical global mesh optimization smoothing algorithm, the error at each step is usually defined by the residual mean square of the positional disturbance of displaced mesh nodes. For a mesh where M nodes get moved to fix the quality of N elements, the global error norm for the l -th iteration of the mesh can be expressed as

$$\varepsilon_l = \sum_{k=1}^M (\mathbf{x}_{k\ opt} - \mathbf{x}_{k\ 0})^2 / M \tag{30}$$

For an error norm of 1%, the global solution for the optimization smoother is assumed to have converged when the following criterion is met

$$|\varepsilon_l - \varepsilon_{l-1}| < 0.01 \varepsilon_l \tag{31}$$

Fig. 5 depicts a very typical solution convergence pattern with 437 initial element failures to begin with. An asymptotic convergence pattern reaches steady state by iteration 8. Fig. 6 describes via a colour contour plot the change in the element angles across smoothing iterations and their relation to the EQM.

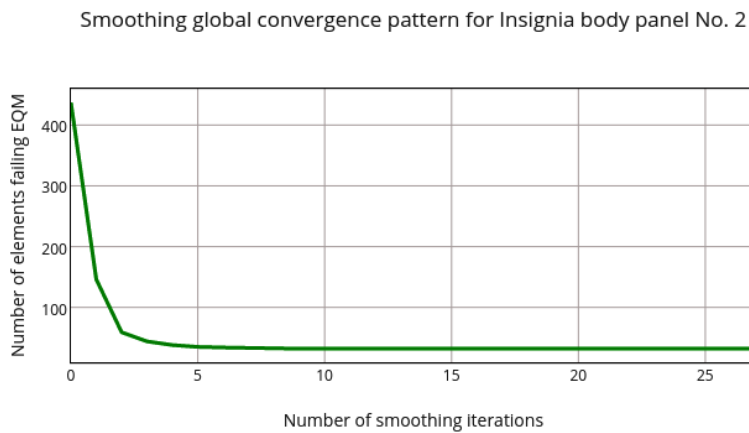


Fig. 5. Optimization smoothing convergence pattern showing EQM failures (EQM limit = 0.45) versus number of iterations

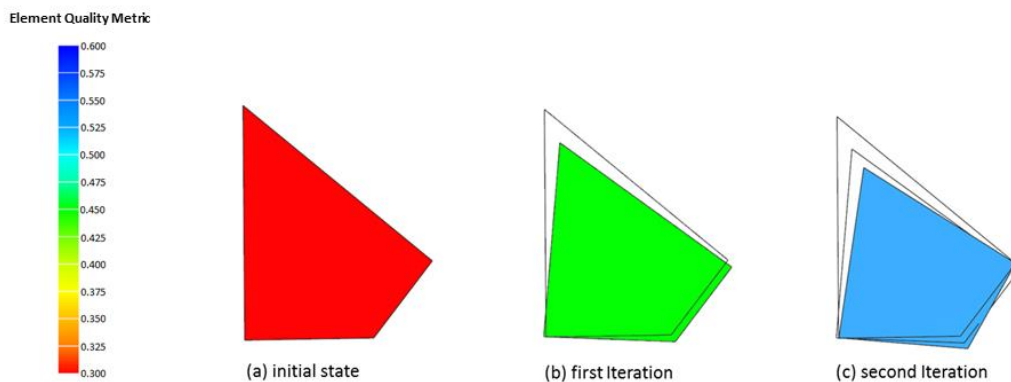


Fig. 6. Variation of element angles with EQM.

10. Results and discussion

Three large panels of the Insignia assembly shown in Fig. 1 are meshed with and without 3D angle optimization. The meshes are generated at a size of 7.5mm with a MEL = 3mm and GFE = 3mm. The meshes are Quad-dominant with less than 7% triangles. A summary of the results with and without optimization smoothing are compared in

Table 1. For body panel No. 1, 80.88 % of the quadrilateral elements failing either min/max angles or skew or element quality metric (EQM) limit (0.45) are cured by angle smoothing. For panel No. 2, the biggest, the improvement is by 76.7% and for panel No. 3 it is 71.04%. The smoothing solution converges for all problems considered. The elements that still fail cannot be fixed because of the constraints of MEL, GFE, angle bounds and the presence of loads and boundary conditions. This small number of failing elements is usually corrected by local remeshing, quad-splitting and/or manual mesh modification.

Table 1. Comparison of EQM and Max/Min Angle improvements for body panels

Body panel Number	Optimization Smoothing	No.of Elements	Element Quality Metric (EQM) failures	Maximum Quad / Tria Angle failures	Minimum Quad / Tria Angle failures	Skew failures	Performance (CPU secs)
1	No	24835	47	89	8	0	
1	Yes	24835	14	11	3	0	1.276
2	No	61482	72	177	25	2	
2	Yes	61482	16	43	8	0	2.70
3	No	40135	70	171	14	5	
3	Yes	40135	14	53	3	2	0.609

Element Size = 8mm; MEL=3mm; GFE=3mm; Element Quality Metric Limit = 0.45; Min/Max Quad Angle Limits = 30°/150°; Skew Limit=30°

Fig. 7 depicts the smoothed mesh on body panel No. 1 showing a total of 19 elements (highlighted in red) failing either or all of the four checks performed. The same for body panel No. 2 are described in Fig.8 with overall 50 elements failing any of the checks. Fig.9 covers panel No. 3 with 55 failing elements. Fig. 10 presents zoomed-in views of certain parts of the meshes in these panels where element angles have been repaired. The images with blue elements are meshes before optimization smoothing. Elements failing angles are boundary-traced in red. Figures 10a and 10c underline trivalent quadrilateral nodes where included angle failure occurs. Typically, trivalent and pentavalent (or higher) nodes in a quadrilateral mesh are the most sensitive connection sites for included angle bounds. Figures 10b and 10d show the corrected states of these angles when subjected to optimization smoothing.

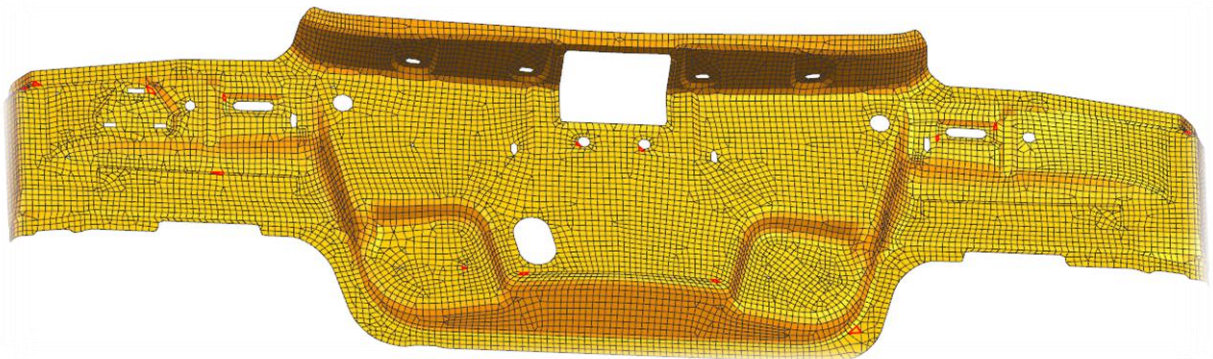


Fig. 7. Body panel (No. 1) meshed with angle optimization smoothing (19 failures shown in red).

Fig. 11 provides a close-up of an embossed section of the mesh from body panel No.2. As before, the blue mesh represents the mesh before smoothing while the golden mesh is optimization-smoothed. A chunk of quadrilateral elements, both isolated and clustered, with a variety of connection styles are all angle-fixed by the angle smoother as is evident in Fig. 11b.

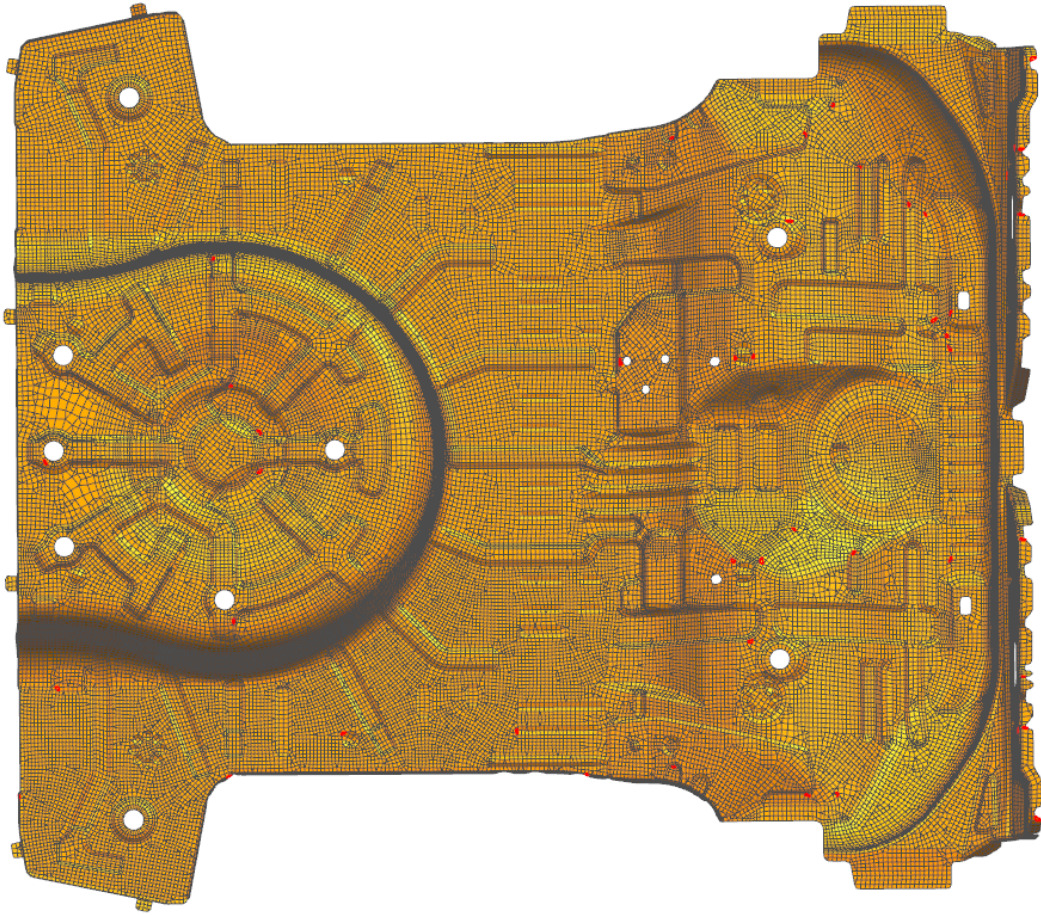


Fig. 8. Body panel (No. 2) meshed with angle optimization smoothing (50 failures shown in red).

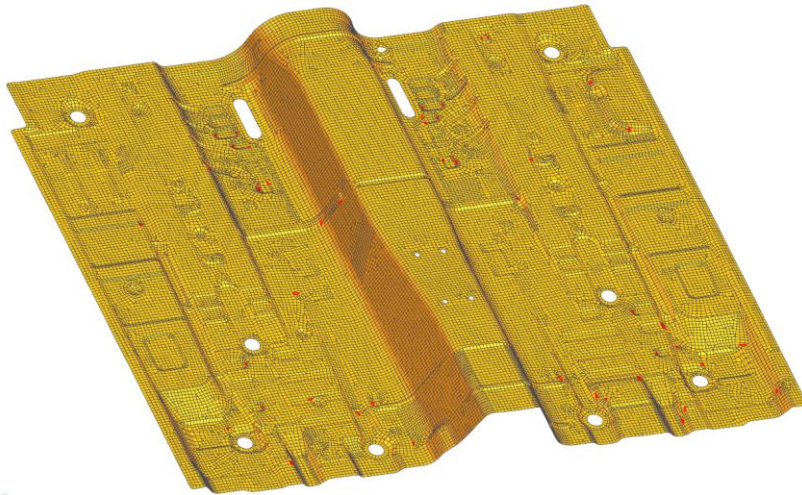


Fig. 9. Body panel (No. 3) meshed with angle optimization smoothing (55 failures shown in red).

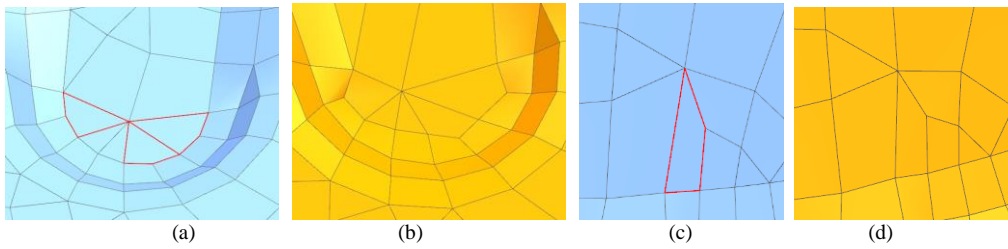


Fig. 10. Details of body panel (No. 2) showing how certain angle failures have been resolved by optimization smoothing.

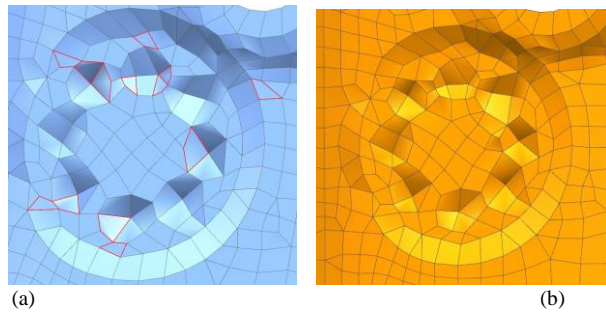


Fig. 11. More details of Body panel (No. 2) showing fixes made with angle optimization smoothing.

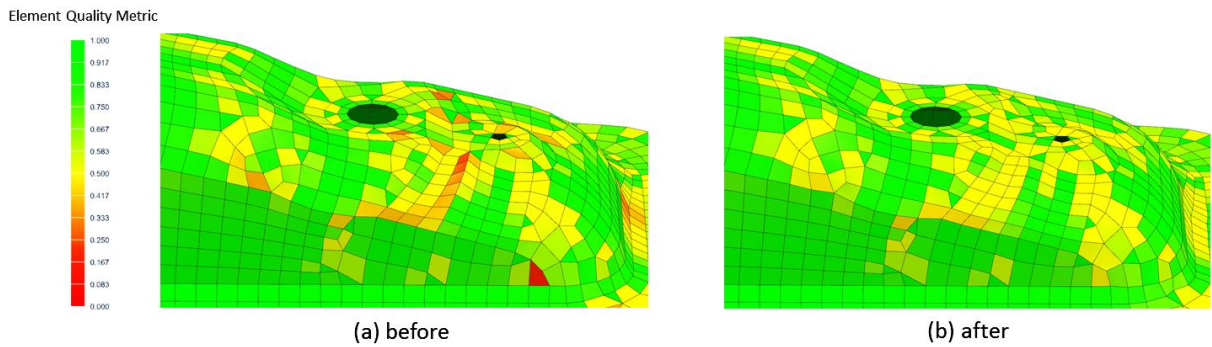


Fig. 12. A sectional detail of Body panel (No. 3) showing the effect of optimization smoothing.

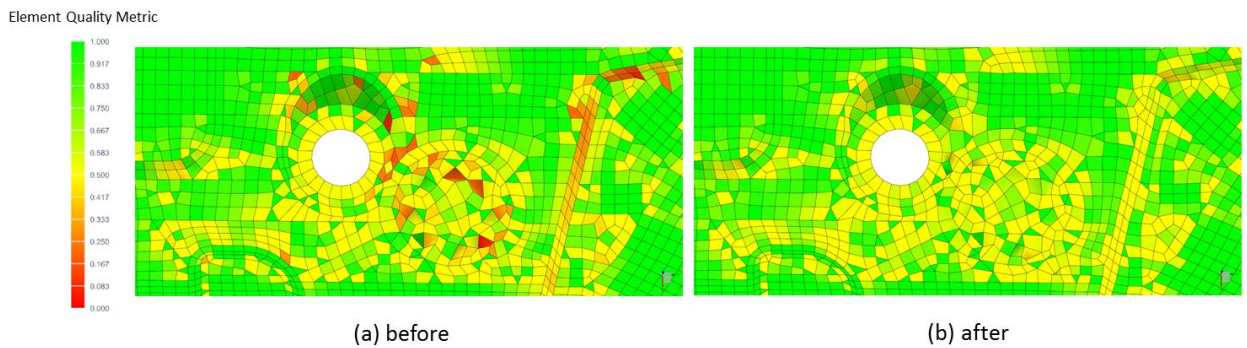


Fig. 13. EQM plot of a sectional detail of Body panel (No. 2) before optimization smoothing.

Fig 12 shows another section (of body panel No. 3) before and after optimization smoothing. It is clearly evident

that several distorted quadrilateral elements are angle-corrected thereby enhancing nearly all of the quality metrics tracked in the section. Fig 13 shows the effect of optimization smoothing on EQM on another section from a different body panel.

On dual core processors (Intel(R) Xeon(R) CPU E3-1270 v5 @ 3.60 GHz) with a 32 GB RAM with Windows 7 Enterprise OS, the cpu seconds consumed by optimization smoothing for the three Insignia body panels are listed in the rightmost column of Table 1. Optimization smoothing time, at its most expensive, is less than 23% of the total time for mesh generation from loading geometry to storing mesh and geometry association data to the database.

11. Conclusion

In this paper, a constrained angle-based optimization smoother is proposed for 3D quadrilateral or quad-dominant BIW meshes. The smoother is developed as a 3D mesh post-processor. Its main objective is to minimize the collective distortion energy of the mesh resulting from element angular deviation from acceptable angular limits. An objective or cost function is constructed to represent the deviation of 3D element angle from a target optimum. This cost function is first locally minimized for each failing element by perturbing along the angle gradient of each failing included angle. A global error norm, computed from the collective displacement of the entire mesh is used to control solution convergence. A non-dimensional element quality metric (EQM) is used to control the smoother. As constraints the optimization smoother uses two criteria, namely minimum element edge length (MEL) and geometry fidelity envelope (GFE). Results of optimization smoothing on several industrial size automotive carbody panels clearly indicate the robustness, benefits and efficacy of the proposed algorithm.

Acknowledgements

The authors cordially thank Mary Otte, development manager of the Meshing & Abstraction group at Digital Factory, Siemens for her encouragement and support at all stages of this investigation.

References

- [1] V. Parthasarathy and S. Kodiyalam, A constrained optimization approach to finite element mesh smoothing, *Finite Elements in Analysis and Design*, 9 (1991), pp. 309-320.
- [2] L. Freitag, On Combining Laplacian and Optimization-based Mesh Smoothing Techniques, *AMD Trends in Unstructured Mesh Generation*, 220 (1997) pp.37-43.
- [3] S. A. Canann, J. R. Tristano, and M. L. Staten, An Approach to Combined Laplacian and Optimization-Based Smoothing for Triangular, Quadrilateral, and Quad-Dominant Meshes, *Proc. 7th Int. Meshing Roundtable*, 1998, pp. 309-323.
- [4] T. Zhou and K. Shimada, An Angle-based Approach to Two-dimensional Mesh Smoothing, *Proc. 9th Int. Meshing Roundtable*, 2000, pp. 373-384.
- [5] H. Xu and T. S. Newman, An angle-based optimization approach for 2D finite element mesh smoothing. *Finite Elements in Analysis and Design*, 42 (2006), pp. 1150-1164.
- [6] P. Knupp, Achieving finite element mesh quality via optimization of the Jacobian matrix norm and associated quantities. Part I - a framework for surface mesh optimization, *Int. J. Numerical Methods in Engg.* 48 (2000) pp. 401-420.
- [7] P. Knupp, Achieving finite element mesh quality via optimization of the Jacobian matrix norm and associated quantities. Part II - a framework for volume mesh optimization and condition number of the Jacobian matrix, *Int. J. Numerical Methods in Engg.* 48 (2000) pp. 1165-1185.
- [8] R.V. Garimella, M.J. Sashkov and P. Knupp, Triangular and Quadrilateral Surface Mesh Quality Optimization Using Local Parametrization, *Computer Methods in Applied Mechanics and Engineering*, 193, (2004), pp. 913-928.
- [9] N. Mukherjee, A hybrid, variational 3D smoother for orphaned shell meshes, *Proc. 11th Int. Meshing Roundtable*, 2002, pp. 379-390.
- [10] S. Owen, Parallel smoothing for grid based methods, *Proc. 21th Int. Meshing Roundtable*, 2012.